The electron–phonon coupling at the Mo(112) surface

2010 J. Phys.: Condens. Matter 22 245501

(http://iopscience.iop.org/0953-8984/22/24/245501)

J. Phys.: Condens. Matter **22** (2010) 245501 (7pp) doi:10.1088/0953-8984/22/24/245501

The electron–phonon coupling at the Mo(112) surface

Ning Wu[1], **Ya B Losovyj**[1,2], **Keisuke Fukutani**[1] **and P A Dowben**[1,3]

[1] Department of Physics and Astronomy and the Nebraska Center for Materials and Nanoscience, University of Nebraska-Lincoln, Lincoln, NE 68588-0111, USA
[2] The J Bennett Johnston Sr Center for Advanced Microstructures and Devices, Louisiana State University, 6980 Jefferson Highway, Baton Rouge, LA 70806, USA

E-mail: pdowben@unl.edu

Received 1 April 2010, in final form 26 April 2010
Published 26 May 2010
Online at stacks.iop.org/JPhysCM/22/245501

Abstract
We investigated the electron–phonon coupling (EPC), in the vicinity of the Fermi level, for the surface-weighted states of Mo(112) from high resolution angle-resolved photoemission data taken parallel to the surface corrugation (i.e. $\langle \bar{1}\bar{1}1 \rangle$). The surface-weighted bandwidth may be discussed in terms of electron–electron interactions, electron impurity scattering and electron–phonon coupling and exhibits a mass enhancement factor $\lambda = 0.42$, within the Debye model, determined from the experimentally derived self-energy. Gold overlayers suppress the mass enhancement of the Mo(112) surface-weighted band crossing the Fermi level at 0.54 $Å^{-1}$.

1. Introduction

There is now a large body of evidence that electron–phonon coupling can affect the band structure, particularly in the region of the Fermi level [1–3]. The resulting mass enhancement factors have not only now been characterized for a whole host of metal surfaces [1], but also for the surfaces of a semimetal like graphite [4] and the surface of a superconductor like 2H-NbS_2 [5]. As noted in a recent review of Mo(112) [6], there is a strong interplay between the surface band structure and the surface structure, where both are affected by the electron–phonon coupling and the wavevector-dependent surface phonon density.

While electron–phonon coupling has been seen to lead to significant mass enhancement for bands in the region of the Fermi level for the Mo(110) surface [3], the Mo(112) has a very significant surface layer spacing relaxation, with a significant oscillatory layer spacer extending at least five layers from the surface into the bulk [6]. The relation of surface layers, for Mo(112) [6], is, in fact, very similar to the strong surface layer relaxation that includes several layers in the surface region of Be(0001) [7–12], where the effective mass enhancement factor of the surface state in the vicinity of the Fermi level is seen to be anisotropic and dependent upon crystal direction [13].

[3] Address for correspondence: Department of Physics and Astronomy, Nebraska Center for Materials and Nanoscience, Theodore Jorgensen Hall - Physical Science Building, 855 North 16th Street, University of Nebraska-Lincoln, NE 68588-0299, USA.

Angle-resolved photoemission spectroscopy (ARPES) [1, 3–5, 13–24], along with high resolution electron energy loss [25] and scanning tunneling spectroscopy [26], are attractive techniques for investigating electron–phonon coupling providing useful information about the real and imaginary parts of the self-energy as well as the mass enhancement factor. The mass enhancement factor λ can be estimated from the temperature-dependent band structure near the Fermi energy [14–20], as would typically be done with high resolution electron energy loss [25] and scanning tunneling spectroscopy [26]. Another approach, favored here, is to extract the mass enhancement factor λ from the shape of the real part of self-energy at the Fermi level or fitting the self-energy with the Debye model [3, 13, 21–23]. Another more sophisticated way is to directly extract the Eliashberg function from high resolution ARPES and λ can be derived from the integral of the Eliashberg function [1, 24]. The advantage of this method is that the Eliashberg function is not temperature-dependent and the dominant phonon modes may be obtained as well.

2. Experimental details

The Mo(112) surfaces, schematically shown in figure 1, were prepared by using standard methods of flashing and annealing in oxygen [6, 27–37], and the surface order characterized by LEED [6]. The high resolution angle-resolved photoemission studies were carried out on the 3 m normal incidence

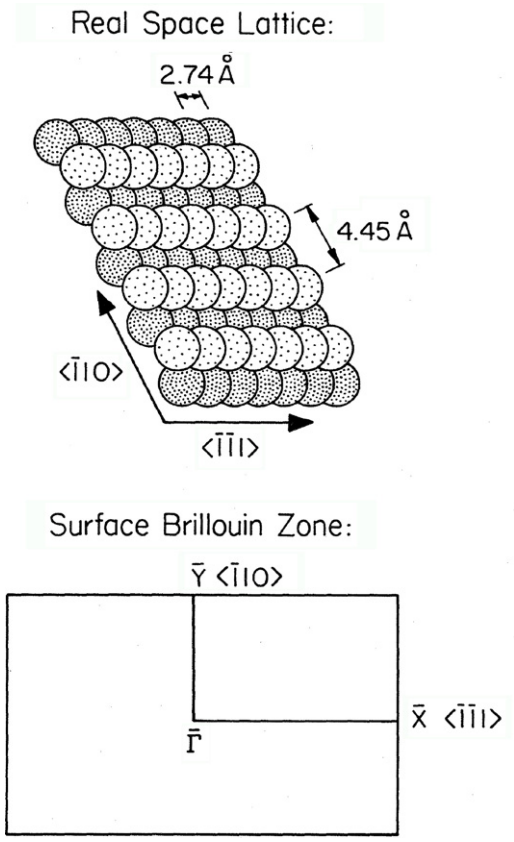

Figure 1. A schematic of the rectangular surface structure of unreconstructed Mo(112).

monochromator (NIM) beamline with a 70 mrad acceptance angle of horizontal radiation from a dipole magnet at the Centre for Advanced Microstructures and Devices (CAMD) synchrotron, as described elsewhere [38]. The normal incidence monochromator is combined with an angle-resolved ultraviolet photoemission spectroscopy (ARUPS) endstation (Scienta SES2002 electron energy analyzer) with a combined resolution of less than 15 meV at about 30 K [38]. The photoemission spectra taken here are for a photon energy of 18 eV, resulting in an improved wavevector resolution because of the lower photon energy. All binding energies are referenced to the Fermi level. The acceptance angle of our electron analyzer is about 8°, with an error in angle of about 0.3°, as is typical of such measurements [3, 5], thus translating to an uncertainty of no more than ± 0.01 Å^{-1} in wavevector resolution along the surface. Though there may be other systematic errors adding to the uncertainty in the wavevector, these errors do not significantly affect estimates of the real and imaginary parts of the self-energy.

The band dispersion along the high symmetry line $\bar{\Gamma}$–$\bar{\mathrm{X}}$ ($\langle\bar{1}\bar{1}1\rangle$ direction of the surface, schematically shown in figure 1), in the whole surface Brillouin zone can be achieved by rotating the sample along its polar axis.

3. Electron–phonon coupling at the Mo(112) surface

Figure 2 shows the $k_\parallel$-dependent quasi-particle band structure along the $\bar{\Gamma}$–$\bar{\mathrm{X}}$ direction (along the surface $\langle\bar{1}\bar{1}1\rangle$ direction) of

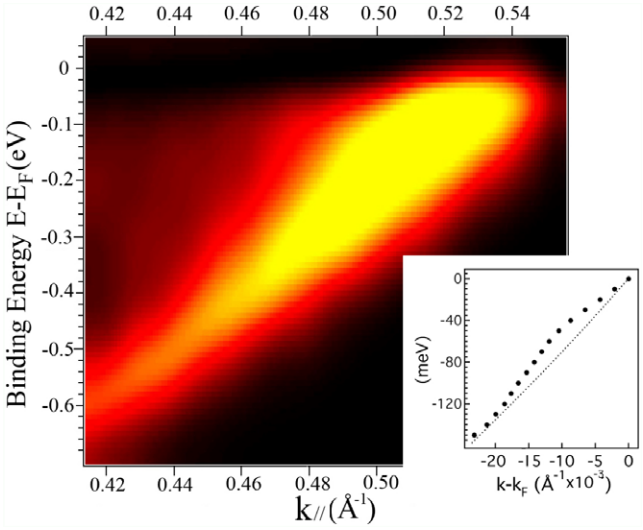

Figure 2. The Mo(112) surface-weighted state band dispersion, at roughly 0.54 Å^{-1} along the $\bar{\Gamma}$–$\bar{\mathrm{X}}$, in the vicinity of the Fermi energy, from high resolution angle-resolved photoemission. Quasi-particle band dispersion extracted from MDCs is shown in the inset, where the dashed line shows the free-electron-like expected parabolic band dispersion.

the Mo(112) surface where a strongly surface-weighted band crosses the Fermi level in the region of 0.54 Å^{-1}. To better illustrate the increase in the effective mass due to the electron–phonon coupling in this region of the Fermi level, only a small region of the surface Brillouin zone from 0.26 to 0.61 Å^{-1} has been plotted out. The inset to figure 2 shows the quasi-particle band dispersion extracted from momentum distribution curves within a 150 meV region below the Fermi level, and the dashed line represents the bare parabolic quasi-'free' electron-like fitting of the band dispersion without consideration of the self-energy. With the high energy and wavevector resolution, the phonon–electron-induced mass enhancement kink in the band structure, in the vicinity of the Fermi energy, is clearly significant and obviously identified in this surface band without any fitting procedures [6].

The angle-resolved photoemission spectroscopy (ARPES) spectral shape may be characterized by the single-particle spectral function $A(\omega, k)$ [3, 21–23]:

$$A(\omega, k) = \frac{\pi^{-1}|\Sigma_{\mathrm{I}}(\omega, k)|}{[\hbar\omega - \varepsilon_k^0 - \Sigma_{\mathrm{R}}(\omega, k)]^2 + \Sigma_{\mathrm{I}}(\omega, k)^2} \qquad (1)$$

where ε_k^0 represents the non-interacting binding energy, and $\Sigma_R(\omega, k)$ and $\Sigma_I(\omega, k)$ are the real part and imaginary part of the self-energy, respectively. Both the real and imaginary parts of the self-energy should ideally be described as functions of electron energy $\hbar\omega$, wavevector k and temperature, which is not included in the ground state formulation of equation (1).

The quantitative analysis of the dependence of the spectral function $A(\omega, k)$ on both wavevector and electron energy has been made using both the energy distribution curve (EDC) mode and momentum distribution curve (MDC) mode. In other words, the energy–momentum plot (figure 2) has been

cut either vertically to get energy distribution curves at various wavevectors or horizontally to get momentum distribution curves at various energies. Since the photoemission signal is also dependent on the Fermi distribution function $f(\omega)$, the MDC (cuts at certain energy so that ω is fixed) tends to be preferable. Furthermore, strong electron–phonon coupling may not only create the mass enhancement kink in the band structure, but also can alter the peak shape of the spectra in EDC mode within 100 meV of the Fermi level [21, 39]. The theory suggests that the effect of multiple scattering of electrons with phonons could complicate the spectral shape near the Fermi level, creating a double-peaked Lorentzian function in EDC mode.

In figure 3, the real part (a) and imaginary part (b) of the self-energy have been plotted, as experimentally extracted from the surface-weighted state band dispersion in the vicinity of the Fermi level from the momentum distribution curves. The real part of the self-energy $\Sigma_R(\omega)$ can be estimated from the experimental Lorentzian peak position $\hbar\omega$ using the relationship

$$\Sigma_R(\omega) = \hbar\omega - \varepsilon_k^0, \tag{2a}$$

where ε_k^0 represents the non-interacting binding energy. Rather than simply using a linear dispersion relationship, we used a more free-electron-like relationship $\varepsilon_k^0 = \hbar v_F(k - k_F) + \beta(k - k_F)^2$ to approximate this bare quasi-particle band dispersion [21, 24]. The value of ε_k^0 is very sensitive to the choice of Fermi vector and, in this case, the Fermi vector has been determined to be 0.539 Å^{-1} from the best fits to the experimental data and theory [6]. From our best fits to the experimental band structure data, we find that $\hbar v_F = 7.27$ eV Å and $\beta = 24.6$ eV Å^2 (as illustrated in the inset of figure 2). The imaginary part of the self-energy was extracted from the Lorentzian curve widths (δk) of the experimental band structure data. From the momentum distribution curves, δE was determined using

$$|2\Sigma\,\mathrm{Im}(\varepsilon)| = \delta E = v\delta k = (\mathrm{d}E/\mathrm{d}k)\delta k, \tag{2b}$$

where v is the 'band'-dependent electron velocity [22, 23], effectively the differential of binding energy versus k vector. Since parabolic dispersion is expected in the free electron model, and even more complex in reality, this velocity is k-dependent rather than simply a constant Fermi velocity.

The easiest way to obtain the mass enhancement factor λ is to calculate the slope of the real part of the self-energy at the Fermi level [1]:

$$\lambda = -\mathrm{d}\Sigma_R(\omega_F)/\mathrm{d}\omega. \tag{3}$$

The simple line fitting indicates that the mass enhancement factor λ is 0.49 ± 0.03. Nevertheless, the problem of this procedure is the difficulty of measuring the slope of the experimental band dispersion right at the Fermi level. This simplified procedure also suffers from the need for finite-temperature corrections and complications of temperature dependence as occurs with a Debye model fitting, a point noted again later.

Another method for extracting the mass enhancement factor is to compare the calculated self-energy based on the

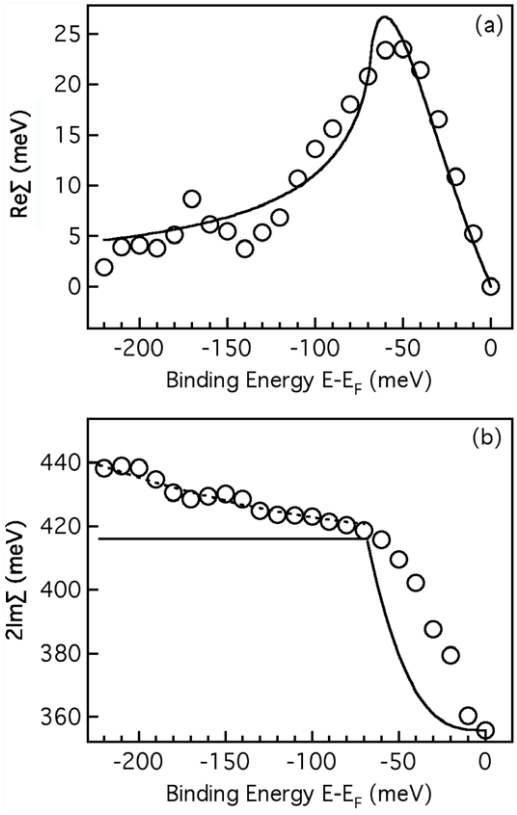

Figure 3. The real part (a) and imaginary part (b) of self-energy Σ determined from fittings of the experimental momentum distribution curves (MDC) obtained from high resolution angle-resolved photoemission. The solid lines are from a Debye model fitting of the data with the mass enhancement factor $\lambda = 0.42$ and the Debye energy of $\hbar\omega_D = 68.34$ meV. The dashed line in imaginary part (b) of self-energy is a parabolic fitting based on model contributions from electron–electron interaction.

Debye model with the experimentally derived real part of the self-energy $\Sigma_R(\omega)$ [21, 22]. In the Debye model, phonon energy is proportional to the wavevector and is cut off at the Debye energy. We obtained the electron–phonon coupling parameter λ and the Debye energy ω_D by fitting the real part of the experimental band dispersion data according to the zero-temperature Debye model, but neglected the wavevector k dependence. In this latter case, the Eliashberg function can be described as [1, 21]

$$\alpha^2 F(\omega) = \begin{cases} \lambda\left(\dfrac{\omega}{\omega_D}\right)^2 & |\omega| < \omega_D \\ 0 & |\omega| > \omega_D \end{cases} \tag{4}$$

where ω is the electron energy and ω_D is the Debye energy. Both mass enhancement factor λ and Debye energy ω_D are involved and determined in the fitting procedure. By using the Eliashberg function above, the self-energy in the zero-temperature Debye model can be written as [21]

$$\mathrm{Re}\,\Sigma = -\left(\frac{\lambda\hbar\omega_D}{3}\right)\left[\left(\frac{\omega}{\omega_D}\right)^3 \ln\left|\frac{\omega_D^2 - \omega^2}{\omega^2}\right| + \ln\left|\frac{\omega_D + \omega}{\omega_D - \omega}\right| + \frac{\omega}{\omega_D}\right]. \tag{5}$$

We rechecked the electron–phonon coupling parameter λ and the Debye energy $\hbar\omega_D$ parameters by fitting the imaginary part of the self-energy, as again both the mass enhancement factor λ and Debye energy ω_D are involved:

$$\mathrm{Im}\,\Sigma = \begin{cases} \dfrac{\pi\lambda\hbar|\omega|^3}{3\omega_D^2} & |\omega| < \omega_D \\ \dfrac{\pi\lambda\hbar\omega_D}{3} & |\omega| > \omega_D. \end{cases} \quad (6)$$

The Debye model indicates that the Debye energy is a little larger than the peak position in $\mathrm{Re}\,\Sigma(\omega)$ and the imaginary part curve resembles a 'step' function and saturates at the Debye energy. The solid line in figure 3(a) indicates the fitting using the Debye model. Though relatively simplistic, the Debye model provides a reasonable fit, especially in the region of mass enhancement in both real and imaginary parts of the self-energy. From the Debye model fittings, we obtain $\lambda = 0.42 \pm 0.02$ and $\hbar\omega_D = 68.34$ meV. The error is estimated from the quality of the fit of the Debye model with the data. The mass enhancement factor $\lambda = 0.42$ derived for the Mo(110) surface [3] is within the experimental error of these results for Mo(112). We conclude that application of the Debye model, even at room temperature, is actually acceptable and that the mass enhancement in the band dispersion of this surface-weighted band originates from strong electron–phonon coupling. Caution should be applied as calculations based on the Debye model show that both the real part and imaginary part are temperature-dependent [1, 14]. Thus the mass enhancement factor λ determined from the real part of the self-energy either with even simplistic fittings or the Debye model is also likely temperature-dependent. The mass enhancement factor λ determined in Debye model calculations decreases with the increase of temperature. Therefore, the true mass enhancement factor λ could be higher than our results indicate here.

The Debye energy, $\hbar\omega_D = 68.34$ meV, derived from Debye model fitting, is much larger than the cutoff of the phonon modes at roughly 33 meV, which is based on the calculated Eliashberg function for bulk molybdenum [40]. Our results indicate that the surface phonon modes not explicitly included in the model could play an important role in this system. Indeed, we expect surface Debye temperature to be much larger than the bulk value [6, 27]. The temperature-dependent photoemission provides support for this contention, as the effective surface Debye temperature measured for Mo(112) is 422 K (i.e. 37–38 meV) [6, 27]. Since electrons are collected at normal emission angle, this is primarily a measure of normal vibrational modes, not in-plane vibrational modes. Therefore, the higher Debye energy implied by the mass enhancement suggests surface in-plane phonon modes contribute significantly to electron–phonon coupling effects seen in the surface band structure.

Our results show a mass enhancement factor for Mo(112) that is similar to that observed with the Mo(110) surface and calculated bulk value. Although, it should be recognized that a direct comparison between Mo(112) and Mo(110) may not be appropriate, as this mass enhancement parameter is dependent on the wavevector, energy and surface. For Mo(112), we have measured the band dispersion along the surface lattice direction where the Mo atoms remain close packed, and in this sense somewhat resembles some of the surface crystallographic directions of Mo(110). Overall, we have found that the determination of Fermi edge and Fermi vector is extremely important to extract the self-energy from ARPES measurement. Slightly different choices for placement of the Fermi edge does not have a profound affect on the estimates of the mass enhancement factor, but obviously can shift the estimates of the Debye energy.

Using equation (6) to generate the fitting of the imaginary part of the self-energy (solid line in figure 3(b)) leads to discrepancies between experiment and fitting that exist both above ω_D and below ω_D. The discrepancies below ω_D, where deviation from the step function is observed, result partly from the temperature dependence of the imaginary part of the self-energy. If the k vector dependence can be neglected, the imaginary part of the self-energy can be defined by [1]

$$\mathrm{Im}\,\Sigma(\omega, T) = \pi \int_0^\infty \mathrm{d}\omega'\, \alpha^2 F(\omega', \omega)[1 - f(\omega - \omega', T) + f(\omega + \omega', T) + 2n(\omega', T)] \quad (7)$$

where f and n are the Fermi and Bose distribution functions, respectively, and ω' is the phonon energy. The temperature dependence of the imaginary part of the self-energy originates from the Fermi and Bose distributions, and this temperature-dependent evolution has been observed for Be [1, 18] and Cu [14]. This deviation from a step function is not surprising for fitting to data taken at finite (room) temperature. The discrepancy above ω_D can be explained by the electron–electron scattering [3, 22]. Otherwise, there is agreement with the derived mass enhancement factor $\lambda = 0.42 \pm 0.02$ and Debye energy $\hbar\omega_D = 68.34$ meV parameters.

We realize that the experiment was taken at room temperature. However, the zero-temperature Debye model we use provides acceptable fits, particularly regarding Debye energy, so long as corrections for finite-temperature effects are made [18], necessitating a shift up in energy by 356 meV, in the bandwidth ($2\Sigma\,\mathrm{Im}(\varepsilon)$), in order to obtain agreement with Debye model fitting at zero temperature. The calculations for Be and Cu show that the bandwidths at zero kelvin can be enhanced at higher temperatures. Given that the imaginary part of the self-energy for Be in the ground state ($E = 0$) can be lifted up in energy by about 200 meV providing a bandwidth of about 400 meV at room temperature [1, 18], the shift of 356 meV necessitated in our study is reasonable. Such temperature-dependent enhancement of bandwidth was observed in Be(0001), where the bandwidth is 352 meV at $T = 330$ K [17] and it decreases significantly to about 100 meV at 40 K [21].

This 356 meV shift in energy is not solely the result of elevated temperature contributions to the electron–phonon-induced broadening. Under the assumption that the scattering mechanisms are independent, except for the electron–phonon scattering, there are two other contributions to the lifetime broadening of the quasi-particle, electron–electron scattering and impurity scattering [3, 22]:

$$\Gamma^\sigma = \Gamma^\sigma_{\mathrm{el-ph}} + \Gamma^\sigma_{\mathrm{el-el}} + \Gamma^\sigma_{\mathrm{impurity}} = 2\,\mathrm{Im}\,\Sigma + \Gamma^\sigma_{\mathrm{el-el}} + \Gamma^\sigma_{\mathrm{impurity}}. \quad (8)$$

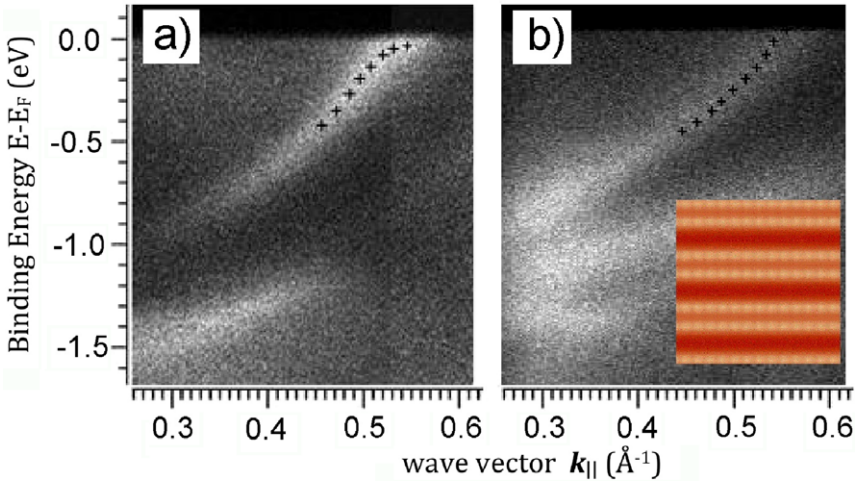

Figure 4. The Mo (112) surface-weighted state band dispersion, at roughly 0.54 Å^{-1} along the $\bar{\Gamma}$–$\bar{X}$, in the vicinity of the Fermi energy before and after deposition of gold. The dispersion for surface-weighted state for the clean surface (a) can be compared to the dispersion following 0.66 monolayers of gold in the ordered $p(1 \times 3)$ missing row Au/Mo(112) structure. The inset illustrates the Fourier transform filtered STM image of the gold (1×3) structure on Mo(112), with periodicity preserved along the rows (furrows) of the Mo(112) substrate. (This figure is in colour only in the electronic version)

All these terms should contribute to the 356 meV shift, required here for Mo(112), although impurity scattering should be independent of temperature. Therefore, a significant fraction of the 356 meV energy shift should come from the impurity scattering, the first term of electron–electron scattering and temperature-induced electron–phonon scattering.

The electron–electron scattering also adds to the bandwidth as $W_{e-e} = 2\beta[(\pi k_B T)^2 + E^2]$, where E is the binding energy [3, 22]. The deviation of the experimental imaginary part of the self-energy from the Debye model fitting, above the Debye energy, is attributed to electron–electron scattering, and may be fitted by a parabolic function. We find that, by making this assumption, the factor $2\beta = 0.417$ eV^{-1} (this fitting is the dashed line in figure 3(b)). Under the Born approximation $2\beta = (\pi U^2)/(2W^3)$, so if we take the Coulomb repulsion $U = 0.6$ eV predicted for Mo [3, 41], then W (the energy difference between the bottom of the occupied part of the surface band and Fermi level) should be about 1.11 eV. This value for the occupied bandwidth is consistent with band structure calculations, which suggest a value close to 1 eV [6], and previous photoemission band structure mappings (1.2 eV) [6, 26, 27]. This adds considerable support to the methodology of our analysis.

In our analysis, we have assumed that the phonon density of states at low energies follows the Debye-like behavior, thus the surface phonons are not explicitly included in the Debye model fitting. Even though the Debye model provides the mass enhancement factor and Debye energy, we cannot, from the data and analysis presented here, ascertain the contribution from the Rayleigh surface modes alone, which can be significant [42] and can lead to increases in the mass enhancement factor [1]. This may explain some of the discrepancies between our experimental data and Debye model fitting of the self-energy. Such discrepancies were also seen in the Debye model fitting of Be(0001) [21]. Further work should focus on the extraction of the Eliashberg function from ARPES data and should best include the consideration of different vibrational mode contributions to the electron–phonon coupling. Underpinning this is the need for detailed calculations of phonon dispersion at the (112) surface.

4. Suppression of the electron–phonon coupling

The mass enhancement of the surface-weighted band is suppressed with adsorption of a partial overlay of gold, as illustrated in figure 4. Au [43, 44], like Ag and Be [45], prefers just filling the furrows in the corrugated Mo(112) surface and do not build linear structures with chains normal to furrows, as seen with many other metal overlayers [46]. As a result, the surface periodicity, along the chains, is preserved for many gold coverages [43]. We see in figure 4 that the surface-weighted Mo(112) band intensity is, in fact, suppressed with moderate Au coverage (in this case a missing gold row $p(1\times3)$ structure), but the mass enhancement of the band, near the Fermi level, is largely lost. With the $p(1 \times 3)$ structure the periodicity along the rows is strictly preserved, as indicated in the inset to figure 4. The loss of any mass enhancement is even more evident with one monolayer of gold in the 1×1 structure where the in-plane lattice of the Mo(112) substrate is preserved, in spite of the suppression of the Mo(112) substrate signal. This is not surprising. The electron–phonon coupling mass enhancement factor is much higher at the surface than in the bulk [1, 3], and suppression of the mass enhancement for the bulk bands of Mo(112) should be expected based on the results for Mo(110) [3] where the electron–phonon-mediated mass enhancement factor decreased by about a factor of two [3].

The bulk bands exhibit little mass enhancement in the vicinity of the Fermi level along the $\langle\bar{1}\bar{1}1\rangle$ direction for Mo(112). In fact, little mass enhancement is seen either for the bulk Mo(112) bands, and the surface-weighted bands near

the Fermi level for bands mapped out along the $\langle\bar{1}\bar{1}1\rangle$ direction for Mo(112), following even fractional monolayers of gold deposition. Indeed, we find that the now interface-weighted state (no longer a surface state or surface resonance state) also exhibits little mass enhancement. Although this remains largely an interface state, it appears that only a fraction of a monolayer of gold is necessary to suppress the noticeable mass enhancement of this state. Thus dimensionality considerations alone do not determine the electron–phonon mass enhancement factor.

What needs to be investigated now is whether the gold depresses the Debye temperature so significantly that the mass enhancement factor cannot be observed or in fact directly suppresses the mass enhancement factor by suppressing the out-of-plane and the in-plane anharmonic motion [47]. From the dependence of the imaginary part of the self energy with gold coverage, there is good reason to believe that the gold overlayer band structure is itself affected by electron phonon coupling. At issue then is whether gold overlayers suppress the out-of-plane and the in-plane anharmonic motion or the expected changes of the surface layer lattice relaxation [47] and if either effect contributes to the loss of the significant mass enhancement of the surface-weighted bands in the vicinity of the Fermi level. The clean surface is expected to exhibit a significant change of the outermost layer relaxation from -15% [6] to -17% [47] for the clean surface to -11.5% with the absorption of only half a monolayer of gold [47]. We expect that, for a corrugated surface like Mo(112), the mass enhancement factor of the surface state in the vicinity of the Fermi level should be highly anisotropic, as is the case for Be(0001) [13], and gold adsorption could either enhance or suppress this suspected anisotropy in the electron–phonon coupling, though an enhancement of the anisotropy of the electron–phonon coupling is more likely [44].

5. Summary

We have investigated the electron–phonon coupling (EPC), in the vicinity of the Fermi level, for the surface-weighted states of Mo(112) parallel to the surface corrugation The surface-weighted bandwidth may be discussed in terms of electron–electron interactions, electron impurity scattering and electron–phonon coupling and exhibits a mass enhancement factor $\lambda = 0.42 \pm 0.006$, within the Debye model, determined from the experimental self-energy data. The Debye energy $\hbar\omega_{\mathrm{D}} = 68.34$ meV is seen to be consistent with the effective Debye temperature, determined from LEED and temperature-dependent photoemission. The bulk bands along $\langle\bar{1}\bar{1}1\rangle$ exhibit little mass enhancement in the vicinity of the Fermi level and gold overlayers suppress the mass enhancement of the Mo(112) surface-weighted band crossing the Fermi level at 0.54 Å^{-1} along the $\bar{\Gamma}$–$\bar{\mathrm{X}}\langle\bar{1}\bar{1}1\rangle$ direction. For a corrugated surface like Mo(112) (figure 1), the mass enhancement factor of the surface state in the vicinity of the Fermi level should be highly anisotropic.

Acknowledgments

The support of the National Science Foundation through grant nos. CHE-0909580, the Nebraska Research Initiative and the Department of Energy EFRC at Louisiana State University, 'Computational Catalysis and Atomic-Level Synthesis of Materials: Building Effective Catalysts from First Principles' is gratefully acknowledged. The J Bennett Johnston Sr Center for Advanced Microstructures and Devices is supported by the Louisiana Board of Regents. We acknowledge valuable discussions with Dr T Y Chien on the ARPES analysis, and with Professor Ivan Yakovkin on the electronic structure of the band structure of Mo(112) and Au on Mo(112).

References

[1] Plummer E W, Shi J, Tang S-J, Rotenberg E and Kevan S D 2003 *Prog. Surf. Sci.* **74** 251
[2] Nolting W 2009 *Fundamentals of Many-Body Physics: Principles and Methods* (Berlin: Springer) ISBN 978-3-540-71930-4
[3] Valla T, Fedorov A V, Johnson P D and Hulbert S L 1999 *Phys. Rev. Lett.* **83** 2085
[4] Leem C S, Kim C, Park S R, Kim M-K, Choi H J, Kim C, Kim B J, Johnson S, Devereaux T, Ohta T, Bostwick A and Rotenberg E 2009 *Phys. Rev.* B **79** 125438
[5] Valla T, Fedorov A V, Johnson P D, Glans P-A, McGuinness C, Smith K E, Andrei E Y and Berger H 2003 *Phys. Rev. Lett.* **92** 086401
[6] Wu N, Losovyj Ya B, Yu Z, Sabirianov R F, Mei W N, Lozova N, Colón Santana J A and Dowben P A 2009 *J. Phys.: Condens. Matter* **21** 474222
[7] Davis H L, Hannon J B, Ray K B and Plummer E W 1992 *Phys. Rev. Lett.* **68** 2632
[8] Feibelman P J 1992 *Phys. Rev.* B **46** 2532
[9] Chen S P 1992 *Surf. Sci.* **264** L162
[10] Johansson L I, Johansson H I P, Andersen J N, Lundgren E and Nyholm R 1993 *Phys. Rev. Lett.* **71** 2453
[11] Holzwarth N A W and Zeng Y 1995 *Phys. Rev.* B **51** 13653
[12] Vobornik I, Fujii J, Mulazzi M, Panaccione G, Hochstrasser M and Rossi G 2005 *Phys. Rev.* B **72** 165424
[13] Chien T, Rienks E D L, Fuglsang Jensen M, Hofmann P and Plummer E W 2009 *Phys. Rev.* B **80** 241416R
[14] McDougall B A, Balasubramanian T and Jensen E 1995 *Phys. Rev.* B **51** 13891
[15] Matzdorf R, Meister G and Goldmann A 1996 *Phys. Rev.* B **54** 14807
[16] Straube P, Pforte F, Michalke T, Berge K, Gerlach A and Goldmann A 2000 *Phys. Rev.* B **61** 14072
[17] Balasubramanian T, Jensen E, Wu X L and Hulbert S L 1998 *Phys. Rev.* B **57** R6866
[18] Tang S-J, Ismail, Sprunger P T and Plummer E W 2000 *Phys. Rev.* B **65** 235428
[19] Kralj M, Siber A, Pervan P, Milun M, Valla T, Johnson P D and Woodruff D P 2001 *Phys. Rev.* B **64** 085411
[20] Luh D-A, Miller T, Paggel J J and Chiang T-C 2002 *Phys. Rev. Lett.* **88** 256802
[21] Lashell S, Jensen E and Balasubramanian T 2000 *Phys. Rev.* B **61** 2371
[22] Higashiguchi M, Shimada K, Nishiura K, Cui X, Namatame H and Taniguchi M 2005 *J. Electron. Spectrosc. Relat. Phenom* **144–147** 639
[23] Johnson P D, Valla T, Fedorov A, Reisfeld G and Hulbert S L 2000 *SRI99: Synchrotron Radiation Instrumentation: 11th US National Conference*; *AIP Conf. Proc.* **521** 73–80
[24] Shi J, Tang S-J, Wu B, Sprunger P T, Yang W L, Brouet V, Zhou X J, Hussain Z, Shen Z-X, Zhang Z and Plummer E W 2004 *Phys. Rev. Lett.* **92** 186401
[25] Kröger J 2006 *Rep. Prog. Phys.* **69** 899
[26] Echenique P M, Berndt R, Chulkov E V, Fauster Th, Goldmann A and Höfer U 2004 *Surf. Sci. Rep.* **52** 219

[27] Waldfried C, McIloy D N, Zhang J, Dowben P A, Katrich G A and Plummer E W 1996 *Surf. Sci.* **363** 296
[28] McAvoy T, Zhang J, Waldfried C, McIlroy D N, Dowben P A, Zeybek O, Bertrams T and Barrett S D 2000 *Eur. Phys. J.* B **14** 747–55
[29] Yakovkin I N, Zhang J and Dowben P A 2001 *Phys. Rev.* B **63** 115408
[30] Jeong H-K, Komesu T, Yakovkin I N and Dowben P A 2001 *Surf. Sci. Lett.* **494** L773–80
[31] Schroeder T, Zegenhagen J, Magg N, Immaraporn B and Freund F J 2004 *Surf. Sci.* **552** 85
[32] Kaya S, Weissenrieder J, Stacchiola D, Todorova T K, Sierka M, Sauer J, Shaikhutdinov S and Freund H J 2008 *Surf. Sci.* **602** 3338
[33] Yakovkin I N, Kuchowicz M, Szukiewicz R and Kolaczkiewicz J 2006 *Surf. Sci.* **600** L240
[34] Kuchowicz M, Stepanovsky S and Kolaczkiewicz J 2006 *Surf. Sci.* **600** 1600
[35] Fukui K, Aruga T and Iwasawa Y 1993 *Surf. Sci.* **281** 241
[36] Sasaki T, Goto Y, Tero R, Fukui K and Iwasawa Y 2002 *Surf. Sci.* **502** 136
[37] Schroeder T, Giorgi J B, Hammoudeh A, Magg N, Baumer M and Freund H J 2002 *Phys. Rev.* B **65** 115411
[38] Losovyj Y, Morris K, Rosa L, Scott J D and Dowben P 2007 *Nucl. Instrum. Methods Phys. Res.* A **582** 258
[39] Ji K 2005 *Photon Factory News* **23** 12
[40] Savrasov S Y and Savrasov D Y 1996 *Phys. Rev.* B **54** 16487
[41] Harrison W A 1980 *Electronic Structure and the Properties of Solids* (San Francisco, CA: Freeman)
[42] Eiguren A, Hellsing B, Chulkov E V and Echenique P M 2003 *Phys. Rev.* B **67** 235423
[43] Losovyj Ya B, Ketsman I, Lozova N, Scott J, Dowben P A, Yakovkin I N and Zuber S M 2008 *Appl. Surf. Sci.* **254** 4326
[44] Fukutani K, Lozova N, Zuber S M, Dowben P A and Losovyj Ya B 2010 *Appl. Surf. Sci.* **256** 4796–800
[45] Fedorus A and Yakovkin I N 2010 private communication
[46] Yakovkin I N 2001 *J. Nanosci. Nanotechnol.* **1** 357–74
[47] Kiejna A 2006 *Phys. Rev.* B **74** 235429